Simulation of Dry-Spinning Process of Polyimide Fibers

Gang Deng, Qingming Xia, Yuan Xu, Qinghua Zhang

State Key Laboratory of Modification for Chemical Fibers and Polymer Materials, College of Materials Science and Engineering, Donghua University, Shanghai 201620, People's Republic of China

Received 31 July 2008; accepted 9 February 2009
DOI 10.1002/app.30236
Published online 4 May 2009 in Wiley InterScience (www.interscience.wiley.com).

ABSTRACT: As one type of high-performance fibers, the polyimide fibers can be prepared from the precursor polyamic acid via dry-spinning technology. Unlike the dry-spinning process of cellulose acetate fiber or polyurethane fiber, thermal cyclization reaction of the precursor in spinline with high temperature results in the relative complex in the dry-spinning process. However, the spinning process is considered as a steady state due to a slight degree of the imidization reaction from polyamic acid to polyimide, and therefore a one-dimensional model based on White-Metzer viscoelastic constitutive equation is adopted to simulate the formation of the fibers. The changes of solvent mass fraction, temperature, axial velocity, tensile stress, imidization degree, and glass transition temperature of the filament along the spinline were predicted. The effects of spinning parameters on glass transition temperature and imidization degree were thus discussed.
 J Appl Polym Sci 113: 3059–3067, 2009

Key words: polyimide fibers; dry-spinning modeling; imidization degree; simulation

INTRODUCTION

Polyimide fibers are one series of high-performance fibers, possessing advantageous properties of chemical inert, excellent mechanical properties and outstanding thermal stability, and they are thus extensively used in aviation, spaceflight field, and others.[1,2] The fibers can be prepared by one-step or two-step processing methods. In one-step method, the polyimide solution in *m*-cresol or *p*-chlorophenol is used to prepare the fibers via wet spinning or dry-jet wet spinning. Unlike the one-step processing, the precursor polyamic acid (PAA) solution in dimethylformamide (DMF) and N, N-dimethylacetamide (DMAC) is used to prepare polyamic acid fibers in two-step method, and then the precursor fibers were *in situ* transformed to the corresponding polyimide fibers by chemical or thermal cyclization reaction.[3]

Correspondence to: Q. Zhang (qhzhang@dhu.edu.cn).
Contract grant sponsor: NSFC; contract grant number: 50873021.
Contract grant sponsor: Shanghai Rising-Star Program; contract grant number: 06QH14001.
Contract grant sponsor: Program for New Century Excellent Talents in University; contract grant number: NCET-06-0421.
Contract grant sponsor: 863 Plan; contract grant number: 2005AA302H30.
Contract grant sponsor: Shanghai Leading Academic Discipline Project; contract grant number: B603.
Contract grant sponsor: 111 Project; contract grant numbers: 111-2-04, B07024.

Dry-spinning technology of polyimide fibers is a two-step process, in which polyamic acid solution forms the precursor fibers via solvent vaporization in the spinning column with high temperature. The precursor fibers are transformed into polyimide fibers by part cyclization reaction in the heating column and part imidization in postheat treatment.

Dry-spinning model focuses on the solvent mass fraction, temperature, axial velocity, and tensile stress along filament. Fok and Griskey[4] solved the solvent mass balance via experimental method. Ohzawa et al.[5,6] proposed a comprehensive one-dimensional model based on an assumption that tensile stress along filament was a constant. Brazinsky et al.[7] gave a two-dimensional model of cellulose acetate (CA)/acetone and compared their calculations with experimental data. Sano and Nishikawa[8,9] studied dry-spinning mechanism including heat transfer coefficient, air drag, etc., and simulated the spinning process of polyvinyl alcohol by the model in which solvent radial distribution was involved.[10] Based on this model, theoretical calculation for producing CA fiber was given.[11] All of the models mentioned above were based on the assumption that spinning drop solutions are Newtonian fluid and the viscoelastic rheological behavior was not considered. Recently, the work on dry-spinning by Gou and McHugh[12,13] presented a modified model with viscoelasticity as well as solidification mechanism. They also developed a two-dimensional model in ternary system, giving more detailed simulation of CA/acetone/water spinning solution.[14,15] For PAA/DMAC spinning system, water mass fraction is less than 0.3%, so a binary system is adapted for dry-spinning model in this article.

In previous reports, it is easily understood to assume the steady state of the dry-spinning process solution because of no chemical reaction for the spinning dopes, such as the dry-spinning formation of CA/acetone and polyvinyl alcohol/water. However, the polymer for polyamic acid precursor may involves the chemical reaction in a heating column during spinning process. A relative steady state in the dry-spinning process must be assumed to set up modified models and to simulate the spinning process. In our experiment, we found that cyclization reaction degree of polyamic acid during the spinning is very low, and the spinning system can be assumed as a steady state at this spinline from 0 to 120 cm. As the spinline is more than 120 cm, it exists a slight imidization reaction from the precursor to polyimide, the spinning process is still considered as a steady state since the absolute value of the imidization degree is very low. Based on the assumption, we gave a modified model to simulate spinning process of polyimide and calculated the imidization degree of precursor polyamic acid.

MODEL DEVELOPMENT

To calculate more efficiently, some assumptions are proposed as follows:

a. The system is at steady state;
b. The density is a constant;
c. Filament is axial symmetry and the cross-section is circle;
d. Neglect radial variation of the system;
e. Neglect surface tension; and
f. Neglect water in the solvent, so as the produced water by imidization reaction.

Figure 1 shows the schematic diagram of dry-spinning process. Spinneret has many holes in industry practice, but to study the dry-spinning process conveniently, a single filament is adopted for the simulation. The z axis is the traveling direction of filament, an axisymmetric spin stream is extruded from spinneret at the top of cabinet ($z = 0$). A counter hot air is pumped from bottom of spinning cabinet ($z = 10$ m) and exits at the top ($z = 0$).

Continuity equation

Mass variation of spinning drop is attributed to evaporation of solvent. Since the mass of polymer does not lose in the spinning process, mass flow rate of polymer W_P is as follows:

$$\frac{dW_p}{dz} = 0 \tag{1}$$

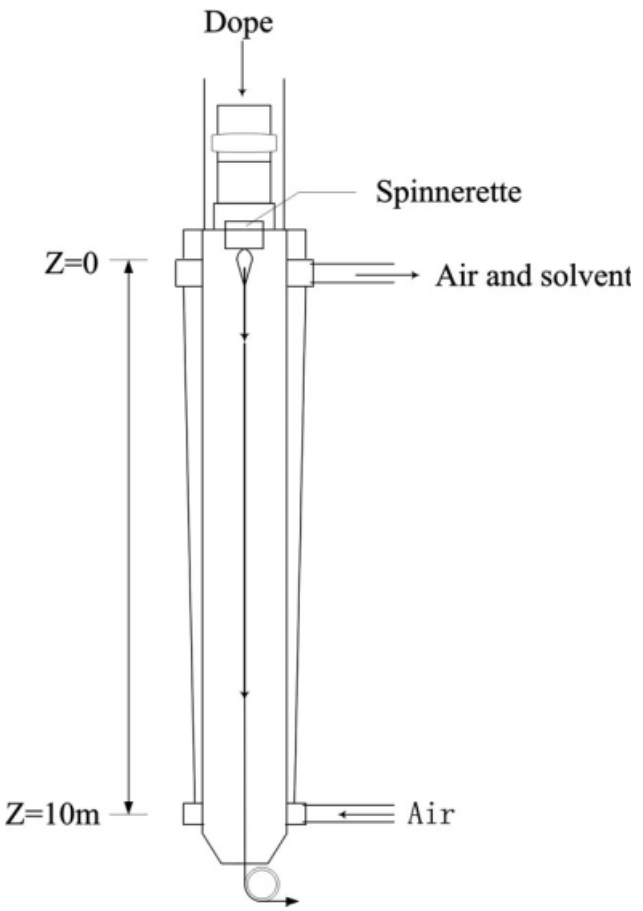

Figure 1 Schematic presentation of dry-spinning process.

For mass flow rate of solvent W_S:

$$W_S = A(z)V(z)\rho w_S(z) \tag{2}$$

$$\frac{dW_S}{dz} = -2\sqrt{\pi A}k_y M_S(y_s - y_0) \tag{3}$$

where A is the cross-section area of filament, V is velocity of threadline, ρ is density of solution, and w_S is mass fraction of the polymer. Combining eqs. (1), (2), and (3) gives the following expression:

$$\frac{dw_S}{dz} + \frac{2\sqrt{\pi A}k_y M_S(y_s - y_0)}{W_P}(1 - w_S)^2 = 0 \tag{4}$$

where w_S is average mass fraction of solvent, k_y is mass transfer coefficient on the gas side of filament surface, y_s is molar fraction of solvent on the gas side of filament surface, y_0 is solvent molar fraction in the bulk gas phase, and M_S is molecular weight of solvent. Molar concentration of solvent on the gas side is calculated by Ohzawa's method:[6]

$$c_S = P_S w_{S,0} \exp(1 - w_{S,0}) \tag{5}$$

$$\ln P_S = 9.9925 - \frac{2750.5}{209.62 + (T + 273.15)} \quad (6)$$

$$w_S = w_{S,0} + 4(w_S^0 - w_{S,0})\mu_1^{-2} \exp\left(-\frac{\mu_1^2 D_{PS} z}{VR^2}\right) \quad (7)$$

where P_S is vapor pressure of solvent, $w_{S,0}$ is solvent mass fraction on filament surface, R is radius of threadline, μ_1 is a constant, D_{PS} is mutual diffusion coefficient, and w_S^0 is initial value of mass fraction. There is no available experimental mutual diffusion coefficient data for PAA/DMAC system, an empirical equation for SPUU/DMAC system is used here.[16]

$$D_{PS} = 8.315 \times 10^{-7} \exp\left[\frac{-14,001\omega_S + 24,809}{8.314(T + 273.15)}\right] \quad (8)$$

Momentum equation

As we know, air drag of filament is related to its surface area. In dry-spinning process, solvent evaporation leads to filament becoming thinner, and therefore the surface area of the filament decreases, which is different from melt-spinning process. The momentum equation of melt-spinning can be used in dry-spinning after modifying the air drag term.[17] Neglecting surface tension, the following momentum equation can be given as

$$\frac{dF}{dz} = \rho A V \frac{dV}{dz} + \pi R C_f \rho_a (V - V_{za})^2 - \rho g A \quad (9)$$

In this equation, F is tension, R is the filament radius, C_f is coefficient of friction drag, ρ_a is the density of air, V_{za} is the counter air flow velocity, and g is acceleration of gravity. The term on left side of the equation is the tension in the filament, and the terms on the right side represent the inertia, air drag, and gravity.

Energy equation

The energy equation is as follows:

$$\rho C_p V_z \frac{dT}{dz} = \frac{2}{R}[h(T_a - T) - \Delta H_v k_y M_s (y_s - y_0)] \quad (10)$$

where h is the convective heat transfer coefficient, T_a is air temperature, T is filament temperature, ΔH_v evaporation heat of the solvent, and C_p is heat capacity of solution. The terms in bracket on right side represent heat transfer between air and filament and evaporation heat of solvent respectively. The term on left side is the total energy variation.

Sano[11] estimated heat transfer coefficient of filament presented by the following equations.

$$Nu = 0.35 + 0.146\left|\mathrm{Re}_P \pm (1.03\mathrm{Re}_w^{0.36} - 0.685)\right|^{0.50} \quad (11)$$

$$\mathrm{Re}_w = 2RV\rho_a/\mu_a \quad (12)$$

$$Nu = 2ah/\lambda \quad (13)$$

$$\mathrm{Re}_P = 2RV_{za}/u_a \quad (14)$$

here Nu is Nusselt number, Re is Reynolds number, and u_a is air viscosity.

Viscoelastic constitutive equation

The previous models were mostly based on Newtonian constitutive equation. However, spinning solutions are non-Newtonian fluid, exhibiting a viscoelastic rheological behavior.[18] We give a viscoelastic constitutive equation based on White-Metzer model in this article. White-Metzer models with the contravariant form can be given as follows:

$$\tau^{ij} + \lambda \frac{\partial \tau^{ij}}{\partial t} = \eta_0 \Delta^{ij} \quad (15)$$

where τ is stress tensor, Δ is strain tensor, λ is relaxation time, and η_0 is zero shear viscosity. Equation (15) further becomes eq. (16)

$$\begin{cases} \tau^{11} - \lambda(2\dot{\varepsilon}\tau^{11}) = 2\eta_0\dot{\varepsilon} \\ \tau^{22} + \lambda(\dot{\varepsilon}\tau^{22}) = -\eta_0\dot{\varepsilon} \\ \tau^{33} + \lambda(\dot{\varepsilon}\tau^{33}) = -\eta_0\dot{\varepsilon} \end{cases} \quad (16)$$

where $\dot{\varepsilon}$ istensile strain rate. After some algebra, eq. (17) can be obtained

$$\begin{cases} \tau^{11} = \frac{2\eta_0\dot{\varepsilon}}{1-2\lambda\dot{\varepsilon}} \\ \tau^{22} = \tau^{33} = \frac{-\eta_0\dot{\varepsilon}}{1+\lambda\dot{\varepsilon}} \end{cases} \quad (17)$$

The definition of elongational viscosity is

$$\eta_e = \frac{\sigma^{11}}{\dot{\varepsilon}} = \frac{\tau^{11} - \tau^{22}}{\dot{\varepsilon}} = \frac{3\eta_0}{(1 - 2\lambda\dot{\varepsilon})(1 + \lambda\dot{\varepsilon})} \quad (18)$$

On the other hand, $\sigma_{11} = F/A$, combining eq. (18), the following equation is obtained:

$$F(1 - 2\lambda\dot{\varepsilon})(1 + 2\lambda\dot{\varepsilon}) = 3\eta_0 A\dot{\varepsilon} \quad (19)$$

For simple extensional flow of 1-D model, tensile strain rate is:

$$\dot{\varepsilon} = \frac{dV}{dz} \quad (20)$$

Relaxation time λ is an important parameter in spinning dynamics, which is related to zero shear viscosity, concentration and temperature of polymer

solution. According to the relaxation time theory of Rouse,[19] an equation of λ can be obtained as follows:

$$\lambda = \frac{6\eta_0 M}{\pi^2 R\rho T(1 - w_S)} \tag{21}$$

Dewitt et al.[20] calculated relaxation time of polyisobutylene/naphthane solution by eq. (21), the result coincides with the experimental value.

Properties of polymer solution

Dry-spinning simulation and related reports for polyamic acid/DMAC system are not published previously, thus part parameters for the models is unknown. Here, we summarize all the parameters as follows.

1. Density—We assume density is a constant, according to ideal mixing rule

$$\frac{1}{\rho} = \frac{w_P}{\rho_P} + \frac{w_S^0}{\rho_S} \tag{22}$$

2. Heat capacity—Neglecting the heat of mixing, heat capacity of solution is expressed as follows:

$$C_P = \phi_p C_{P,p} + \phi_s C_{P,s} \tag{23}$$

3. Evaporation heat

$$\Delta H_v = RT_c T_{b,r}\left(\frac{3.978T_{b,r} - 3.938 + 1.555\ln P_c}{1.07 - T_{b,r}}\right) \tag{24}$$

where T_c is critical temperature, P_c is critical pressure, T_b is atmospheric boiling point, $T_{br} = T_b/T_c$. The calculated result is 13,208 J/mol.[21]

4. Viscosity of polymer solution—Van Krevelen's method[22] is used to estimate zero shear viscosity of PAA/DMAC system.
   a. If temperature is high enough to T_g, $T \geq T_S = 1.2T_g$,

$$\eta_0 = KP_n^m(1 - \omega_s)^n \exp(\Delta E/RT) \tag{25}$$

   In this equation, K, m, and n are constants, η_0 is in poise, ΔE is flow activation energy, P_n is degree of polymerization, R is the universal gas constant, and T is in K.
   b. If temperature is near to T_g or less than T_g, namely, $T_S \geq T \geq T_g$ or $T_g \geq T$

$$\log \eta_0(T) = \log \eta_0(T_S) - \frac{c_1(T - T_S)}{c_2 + (T - T_S)} \tag{26}$$

   where, c_1 and c_2 are constants. For dry-spinning process, eq. (25) is used and we can further get:

$$\ln \eta_0 = \ln A + B\ln(1 - w_S) + C/T \tag{27}$$

According to the rheological date of Yang et al.[23], the calculated parameters of A, B, and C are 1.48, 9, and 943, respectively. For PAA/DMAC system, even though viscosity would reduce due to a slight degradation of PAA at high temperature, the assumption that viscosity of the dope is not affected by this factor, because time that filament stays in spinning path is very short and the degradation can be neglected. Experimental data support this assumption.

5. Glass transition temperature—Glass transition temperature for polymer solution is given by the following equation.

$$T_g = \frac{T_{g,p} + (2.5T_{g,s} - T_{g,p})\phi_s}{1 + 1.5\phi_s} \tag{28}$$

$T_{g,p}$ and $T_{g,s}$ represent glass transition temperatures of polymer and of solvent, respectively. For PAA/DMAC system, glass transition temperature of the polymer is related to imidization degree.[24] The imidization degree of PAA can be calculated by the following equation.[25]

$$\ln(1 - \beta) = -A\exp\left(-\frac{E_a}{RT}\right)t \tag{29}$$

The relation between glass transition temperature and imidization degree of PAA is as follows[24]:

a) $\beta \leq 0.84$,

$$T_{g,p} = 90.4\beta + 128.4 \tag{30}$$

b) $0.84 \leq \beta \leq 0.96$,

$$T_{g,p} = 533.3\beta - 243.68 \tag{31}$$

c) $0.96 \leq \beta$,

$$T_{g,p} \approx Const \tag{32}$$

T_{gs} is estimated by $T_{g,s}/T_m = 2/3$, and here T_m is −20°C.

Properties of quench air

1. Density of air

$$\rho_a = 0.351/T_f \tag{33}$$

Here, T_f is arithmetic mean of filament temperature and quench air temperature.

2. Viscosity of air

$$u_a = \frac{1.446 \times 10^{-5}T_f^{1.5}}{T_f + 113.9} \tag{34}$$

3. Air drag coefficient

$$C_f = 0.68\left[\frac{2R\rho_a(V - V_a)}{\eta_a}\right]^{-0.8} \quad (35)$$

Numerical approach

The computation of dry-spinning model is to solve a set of highly coupled differential equations. Here, fourth order Runga-Kutta algorithm method is used to solve the equations. Considering the swell effect, we adopt initial value of 1.5 as spinneret diameter at $Z = 0$. Since there is no available datum of mass transfer coefficient of PAA/DMAC system, a value of $h/k_y = 8$ cal/(g mol °C) is used. Initial values for the simulation are listed in Table I, and the algorithm procedure is as follows:

1. At $z = 0$, it is difficult to calculate the initial value of filament tension. Gou and McHugh[12] assumed an initial tensile stress between 10^4 and 10^5 dyn/cm^2 (0.1–1 N/cm^2). According to their data, an initial value of filament tension of 0.5 N/cm^2 is assumed in this article. The initial value of temperature and mass fraction is dependent on the solution. The initial values of velocity and radius of filament are calculated by mass flow rate of solution and spinneret diameter. The initial value of imidization degree is 0.05.
2. $(dV/dz)_{z=0}$ is determined by trial and error until filament velocity matching with take-up velocity.[11] In our calculation, the tolerance error is 10^{-3}.

RESULTS AND DISCCUSION

Model prediction

Flash evaporation occurs near the spinneret due to a high temperature difference between solution and heating air flow in the spinning column. As shown in Figure 2, mass fraction of solvent immediately decreases after runout of spinneret. At the beginning, namely near the $z = 0$, high free solvent content inside the filament results in solvent diffusion caused by heat transfer and mass transfer; whereas, when solvent content decrease to near zero at $z >$ 120 cm, the filament completely becomes solid fiber.

TABLE I
Initial Values for the Simulation

Parameters	Values
Temperature (T)	80 °C
Mass fraction of solvent (w_2^0)	30%
Mass flow rate of solution (W)	0.02 g/s
Diameter of spinneret (d)	0.35 mm
Velocity of quench air (V_{az})	50 cm/s
Temperature of quench air (T_a)	250 °C
Length of spinline (L)	1000 cm
Initial imidization degree of PAA (β^0)	0.05
Glass transition temperature of PAA (T_g^0)	−2 °C
Heat capacity of polymer ($C_{p,P}$)	2.1 J/(g °C)
Heat capacity of solvent ($C_{p,S}$)	3.19 J/(g °C)
Take-up velocity(V_L)	350 cm/s
Density of polymer (ρ_1)	1.050 g/cm^3
Density of solvent (ρ_2)	0.937 g/cm^3
Total pressure (P)	1 atm

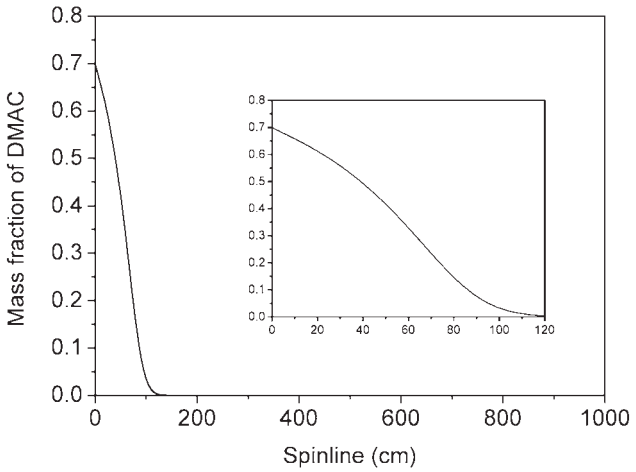

Figure 2 Variation of solvent mass fraction along spinline.

The variation of filament velocity below the spinneret is illustrated in Figure 3. Near the spinneret, the solution flow is easily drawn, leading to the increase of velocity. With the evaporation of the solvent, the filament gradually becomes the viscous flow, and then the solidification of the filament results in an approximately constant velocity of the fibers.

The change of the filament tension along the spinline with air drag and without air drag is shown in Figure 4. Apparently, the two curves sharply increase near the spinneret. The one without air drag soon reaches a plateau because of the

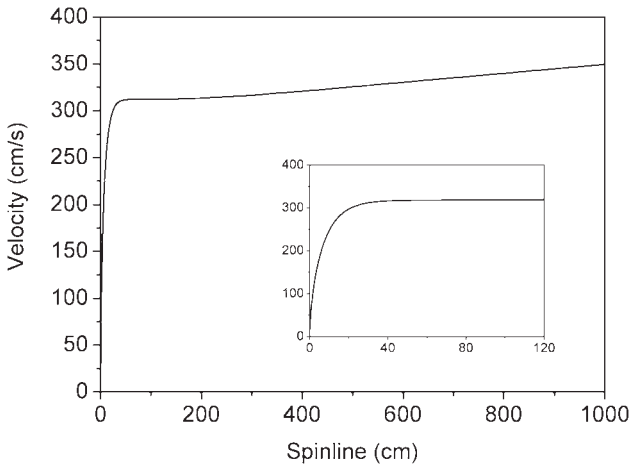

Figure 3 Variation of the filament velocity along spinline.

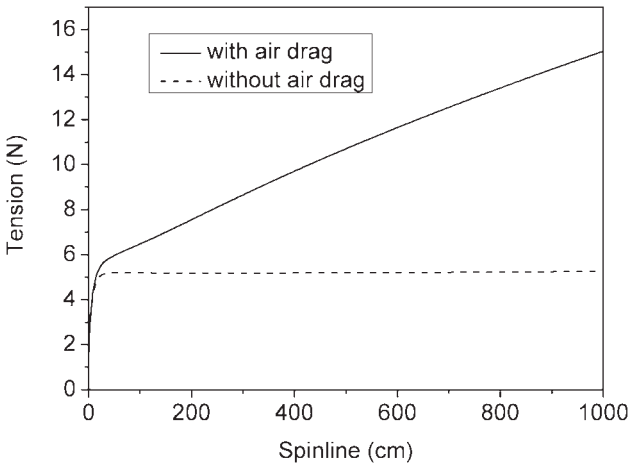

Figure 4 Variation of filament tension along spinline.

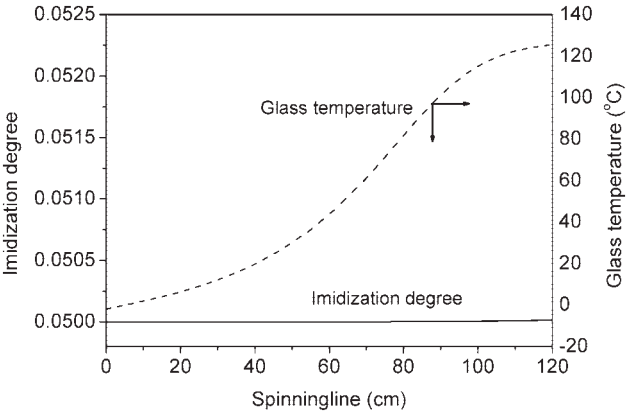

Figure 6 Variation of imidization degree and glass transition temperature.

solidification and the reduced stretchability. The other one with the air drag keeps gradually increasing due to the increasing surface area of filament along the spinning path.

As reported by Kotera et al.[26], solvent content in the solution has an influence on the temperature and imidization degree of the fiber. Therefore, both the temperature and imidization degree of the filament do not obviously increase at the relative high mass fraction of solvent. As shown in Figure 2, mass fraction of the solvent decreased to zero and filament thus solidified at $\sim$ 120 cm. After that, many properties of filament obviously changed, such as filament temperature and imidization degree. To discuss the properties in detail, the spinline is divided into two sections, namely $z < 120$ cm and >120 cm.

Figure 5 shows the temperature change of the filament along the spinline at the first section of $z < 120$ cm. Apparently, the filament temperature decreases from the initial 80°C to $\sim$ 70°C at the spinline of 52 cm due to flash evaporation. As heat transfer between filament and hot air is equal to evaporation heat of solvent, the filament temperature decreases to a minimum value, and then temperature rises quickly.

As shown in Figure 6, imidization degree of the filament does not obviously change due to more solvent in the filament and low temperature at the section of $z < 120$ cm. As solvent quickly evaporated, glass transition temperature (T_g) gradually increases, and the curve is near a plateau at $z = \sim 120$ cm, indicating the glass transition temperature equal to the value of polymer at this time. The T_g of the polymer is related to imidization degree, so the T_g of the filament is mainly dependant on solvent evaporation because of no change of imidization reaction at $z <$ 120 cm.

At the second section of $z > 120$ cm, the filament temperature and imidization degree is very different from the first section. Figure 7 shows the temperature change along the spinline at this section. Apparently, the filament temperature quickly rises due to

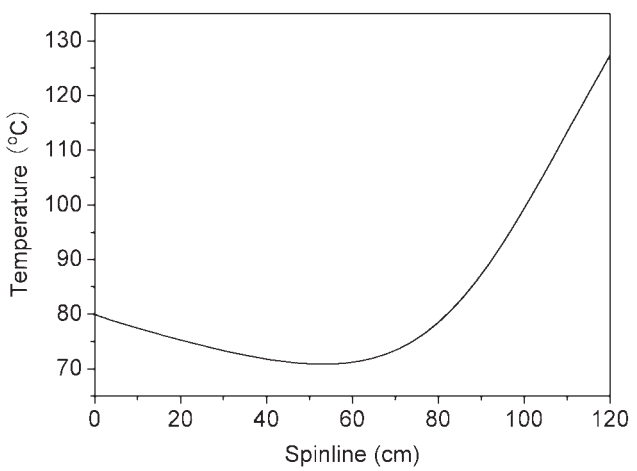

Figure 5 Variation of filament temperature along spinline as $z < 120$ cm.

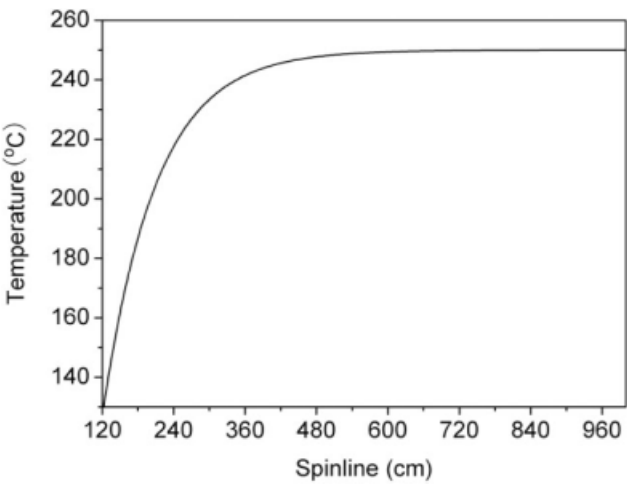

Figure 7 Variation of filament temperature along spinline ($z > 120$ cm).

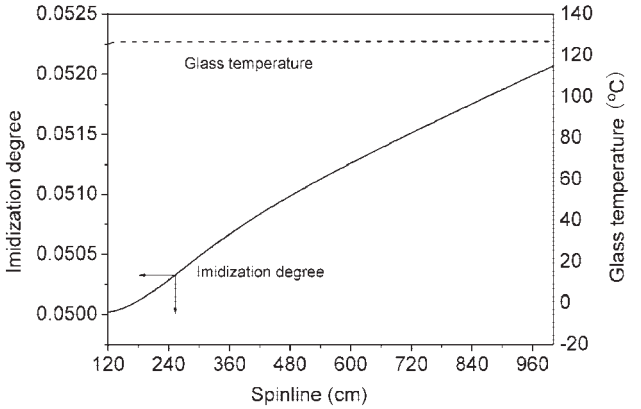

Figure 8 Variation of imidization degree and glass transition temperature along spinline ($z > 120$ cm).

heat transfer and is up to air temperature at $z = \sim 500$ cm. As shown in Figure 8, there exists imidization reaction after solidification of the filament, and imidization degree slightly increased along the spinline, which is different from the first section ($z < 120$ cm). However, the absolute value of imidization degree increases only by 0.18% in the whole spinning path, which conforms to our initial assumption of a low imidization degree. If effect of reaction heat on temperature is considered, eq. (10) can be transformed into the following equation:

$$\rho C_p V_z \frac{dT}{dz} = \frac{2}{R}\left[h(T_a - T) - \Delta H_v k_y M_2 (y_2 - y_0) + \frac{273 W_1 \beta}{V}\right] \quad (36)$$

where, the last term at right side refers to the contribution of the reaction heat, equal to 70.59 kJ/mol at 240°C.[27] As a matter of fact, this contribution of the reaction heat can be neglected since the imidization degree is only 0.18%. Therefore, as calculated by eq. (36), the trend of the filament temperature along

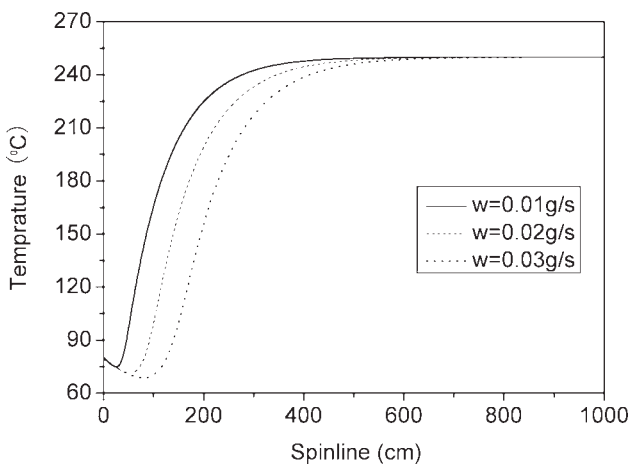

Figure 9 Effect of mass flow rate on filament temperature.

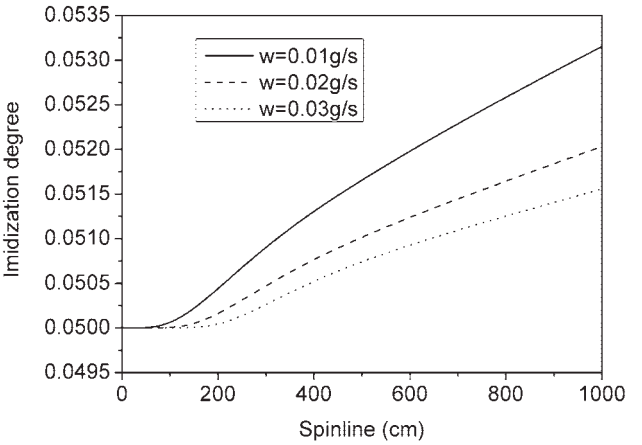

Figure 10 Effect of mass flow rate on imidization degree of the filament.

the spinline with the contribution of the reaction heat is very similar to the Figures 5 and 7. In the second section, glass transition temperature is a plateau due to no solvent in the filament, as shown in Figure 8.

Effect of spinning parameters

The dry-spinning process can be controlled by changes of parameters, such as media temperature and mass flow rate. The effects of mass flow rate and quench air temperature effect on imidization degree and glass transition temperature are discussed below.

As shown in Figure 9, the solidification point shifts to far from the spinneret as increasing mass flow rate. At a fixed spinline, namely at a same z value, the increase in the mass flow rate results in the decrease of the filament temperature. The reason is that more solution flows into the spinning path, which decreases the specific surface area of the filament and thus decreases heat transfer of per unit

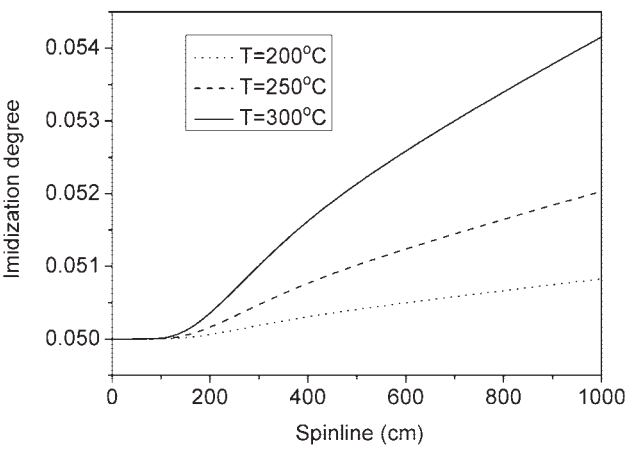

Figure 11 Effect of air temperature on imidization degree.

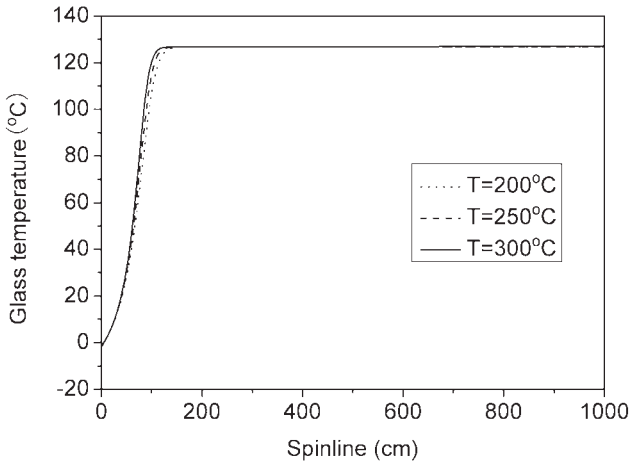

Figure 12 Effect of air temperature on glass transition temperature.

mass. The same reason leads to decreasing imidization degree, as shown in Figure 10.

The media temperature has an influence on imidization degree. As show in Figure 11, increasing air temperature results in relative high imidization reaction rate, leading to the increase in imidization degree. On the other hand, Figure 12 gives the change of the glass transition temperature of the filament with the media temperature, indicating a slight effect of the air temperature on the glass transition temperature due to the change of imidization degree.

CONCLUSIONS

To simulate dry-spinning process of polyimide fibers, assumptions of low imidization degree from the polyamic acid precursor to polyimide and the steady state in the dry-spinning process are proposed. A modified one-dimensional model based on White-Metzer viscoelastic constitutive equation is used to predict the changes of solvent mass fraction, temperature, velocity, and tension of filament along the spinline (z). The results show that the dry-spinning process can be divided into two sections. At first section of $z < 120$ cm, flash evaporation of solvent in the heat-spinning path results in the sharp decrease of the solvent mass fraction, which dominates the formation of the filament. Filament temperature first falls down and then rises up at this section, and the velocity, tension, and glass transition temperature of filament increases along the spinline. Imidization degree does not obviously change in the first section. At section of $z > 120$ cm, on the other hand, mass fraction of solvent is zero and filament becomes a solid one. Velocity and glass transition temperature of the filament are constant along the spinline, whereas there exists a slight increase in imidization degree. Moreover, the spinning parameters have an influence on the formation process. Increasing mass flow rate leads to solidification point moving far from the spinneret and the decrease in imidization degree. Relative high media temperature in the spinning path causes the increasing imidization degree, even though this increasing absolute value is very low.

NOMENCLATURE

A	Cross-section area of filament, cm^{-2}
c_S	Molar concentration of solvent on the gas side, mol/L
C_f	Coefficient of friction drag, (−)
C_p	Heat capacity, J/(g °C)
d	Diameter of spinneret, cm
D_{PS}	Mutual diffusion coefficient
F	Tension, N
g	Acceleration of gravity, m/s^2
h	Heat transfer coefficient, $W/(m^2\ K)$
k_y	Mass transfer coefficient on the gas side, $h/k_y = 8$ cal/(g mol °C)
L	Length of spinline, cm
M	Molecular weight, g/mol
η_0	Zero shear viscosity, Pa s
Nu	Nusselt number, (−)
P_c	Critical pressure, atm
P_n	Degree of polymerization, (−)
P_S	Vapor pressure of solvent, hpa
R	Filament radius, cm
Re	Reynolds number, (−)
T	Temperature, °C
T_b	Atmospheric boiling point, °C
T_{br}	T_b/T_c, (−)
T_c	Critical temperature, °C
T_f	Arithmetic mean of filament temperature and quench air temperature, °C
T_g	Glass transition temperature, °C
T_m	Melting point temperature, °C
V	Velocity of treadline, cm/s
V_L	Take-up velocity, cm/s
V_{za}	Counter air flow velocity, cm/s
w	Mass fraction, (−)
$w_{S,0}$	Solvent mass fraction on filament surface, (−)
w_S^0	Initial Solvent mass fraction of spinning solution, (−)
W	Mass flow rate, g/s
y_0	Solvent molar fraction in the bulk gas phase, (−)
y_s	Molar fraction of solvent on the gas side of filament surface, (−)
β	Imidization degree of PAA, (−)
ρ	Density of solution, g/cm^3
u_a	Air viscosity, Pa s
τ	Stress tensor, Pa

λ	Relaxation time, s
$\dot{\varepsilon}$	Tensile strain rate, s^{-1}
Δ	Strain tensor, (−)
ΔE	Flow activation energy, J/mol
ΔH_v	Heat of evaporation of the solvent per unit mass, J/mol

Subscript and Superscript

P	Polymer
S	Solvent
0	Initial value
z	z direction

References

1. Ding, M. Prog Polym Sci 2007, 32, 623.
2. Zhang, Q.; Dai, M.; Ding, M.; Chen, D.; Gao, L. Euro Polym J 2004, 40, 2487.
3. Zhang, Q.; Dai, M.; Ding, M.; Chen, D.; Gao, L. J Appl Polym Sci 2004, 93, 669.
4. Fok, S. Y.; Griskey, R. G. J Appl Polym Sci 1967, 11, 2417.
5. Ohzawa, Y.; Nagano, Y.; Matsuo, T. J Appl Polym Sci 1969, 13, 257.
6. Ohzawa, Y.; Nagano, Y. J Appl Polym Sci 1970, 14, 1879.
7. Brazinsky, I.; Williams, A. G.; LaNieve, H. L. Polym Eng Sci 1975, 15, 834.
8. Sano, Y.; Nishikawa, S. Kagaku Kougaku 1964, 28, 275.
9. Sano, Y.; Nishikawa, S. Kagaku Kougaku 1965, 29, 294.
10. Sano, Y. Drying Technol 1993, 11, 697.
11. Sano, Y. Drying Technol 2001, 19, 1335.
12. Gou, Z.; McHugh, A. J. J Appl Polym Sci 2003, 87, 2136.
13. Gou, Z.; McHugh, A. J. J Non-Newtonian Fluid 2004, 118, 121.
14. Gou, Z.; McHugh, A. J. Intern Polym Proc 2004, 3, 244.
15. Gou, Z.; McHugh, A. J. Intern Polym Proc 2004, 3, 254.
16. Li, G.; Yamada, T. H. J Polym Eng 2007, 27, 621.
17. Doufas, A. K.; McHugh, A. J.; Miller, C. J Non-Newtonian Fluid 2000, 92, 27.
18. Ziabicki, A. Fundamentals of Fibre Formation, Wiley: New-York, 1976.
19. Rouse, P. E. J Chem Phys 1953, 21, 1272.
20. Dewitt, T. W.; Markovitz, H.; Padden, F. J.; Zapas, L. J. J Colloid Sci 1955, 10, 175.
21. Nicholas, P. C. Handbook of Chemical Engineering Calculations, 3rd ed.; McGraw-Hill: New York, 2004.
22. Van Krevelen, D. W. Properties of Polymers, 3rd ed.; Elsevier: Amsterdam, 1990.
23. Yang, G.; Yu, J.; Yang, T.; Liu, Z. Synth Fiber 2007, 36, 26.
24. Chen, R.; Guo, L.; Wang, W.; Huang, P. China Plast Ind 2005, 33, 32.
25. Huang, P.; Geng, H.; Cheng, R.; Wang, X.; Shi, J. Acta Polym Sinica 2004, 2, 256.
26. Kotera, M.; Nishino, T.; Nakamae, K. Polymer 2000, 41, 3615.
27. Huang, P.; Geng, H.; Liu, J.; Shi, J.; Ma, Z. J Nanjing Univ Tech 2004, 26, 14.